

# *Swift* and optical observations of GRB 050401

Massimiliano De Pasquale<sup>1</sup>, Andy P. Beardmore<sup>2</sup>, S.D. Barthelmy<sup>3</sup>, P. Boyd<sup>3</sup>, D.N. Burrows<sup>4</sup>, R. Fink<sup>3</sup>, N. Gehrels<sup>3</sup>, S. Kobayashi<sup>4,5</sup>, K.O. Mason<sup>1</sup>, R. McNought<sup>6</sup>, J. A. Nousek<sup>4</sup>, K.L. Page<sup>2</sup>, D.M. Palmer<sup>7</sup>, B.A. Peterson<sup>6</sup>, P.A. Price<sup>8</sup>, J. Rich<sup>6</sup>, P. Roming<sup>4</sup>, S.R. Rosen<sup>1</sup>, T. Sakamoto<sup>3</sup>, B.P. Schmidt<sup>6</sup>, J. Tueller<sup>3</sup>, A.A. Wells<sup>2</sup>, S. Zane<sup>1</sup>, B. Zhang<sup>9</sup>, H. Ziaeepour<sup>1</sup>.

<sup>1</sup> Mullard Space Science Laboratory, University College London, Holmbury St. Mary, Dorking Surrey, RH5 6NT, UK; mdp@mssl.ucl.ac.uk

<sup>2</sup> University of Leicester, University Rd, Leicester, LE1 7RH, UK

<sup>3</sup> NASA/Goddard Space Science Flight Center, Greenbelt, MD 20771, USA

<sup>4</sup> Department of Astronomy and Astrophysics, Pennsylvania State University, 525 Davey Laboratory, University Park, PA 16802 USA

<sup>5</sup> Center for Gravitational Wave Physics, Pennsylvania State University, University Park, PA 16802, USA

<sup>6</sup> Research School of Astronomy and Astrophysics, Mount Stromlo Observatory, Cotter Road, Weston Creek, ACT 2611 Australia

<sup>7</sup> Los Alamos National Laboratories, Los Alamos, NM87545 USA

<sup>8</sup> Institute for Astronomy, 2680 Woodlawn Drive, Honolulu, HA96822, USA

<sup>9</sup> Department of Physics, University of Nevada, Las Vegas, NV89154, USA

Accepted...Received...

## ABSTRACT

We present the results of the analysis of  $\gamma$ -ray and X-ray data of GRB 050401 taken with the *Swift* satellite, together with a series of ground-based follow-up optical observations. The *Swift* X-ray light curve shows a clear break at about 4900 s after the GRB. The decay indices before and after the break are consistent with a scenario of continuous injection of radiation from the ‘central engine’ of the GRB to the fireball. Alternatively, this behaviour could result if ejecta are released with a range of Lorentz factors with the slower shells catching up the faster at the afterglow shock position. The two scenarios are observationally indistinguishable.

The GRB 050401 afterglow is quite bright in the X-ray band, but weak in the optical, with an optical to X-ray flux ratio similar to those of ‘dark bursts’. We detect a significant amount of absorption in the X-ray spectrum, with  $N_H = (1.7 \pm 0.2) \times 10^{22} \text{ cm}^{-2}$  at a redshift of  $z = 2.9$ , which is typical of a dense circumburst medium. Such high column density implies an unrealistic optical extinction of 30 magnitudes if we adopt a Galactic extinction law, which would not be consistent with the optical detection of the afterglow. This suggests that the extinction law is different from the Galactic one.

**Key words:** Gamma-Ray Bursts

## 1 INTRODUCTION

Observations of Gamma-Ray Bursts (GRBs) have shown that they are followed by fading X-ray, optical and radio afterglows. These are thought to arise when the burst ejecta interact with the surrounding medium and produce a shock, which propagates in the medium and heats the electrons. The latter, cooling by synchrotron emission, produce the observed radiation. Studies of afterglows can provide invaluable information on the central engine of GRBs and on the circumburst medium, and can possibly distinguish different subclasses in the GRBs population.

Some authors (see e.g. Lazzati et al. 2002 and references therein; Berger et al. 2005 and Lamb et al. 2005

for recent results) have pointed out the existence of a subclass of GRB, whose optical emission is at least  $\sim 2$  magnitude below that of the average of the optically detected bursts. Different models have been proposed to explain these “dark bursts”, ranging from a cosmological origin (Bromm & Loeb 2002; Fruchter 1999) to scenarios where they go off in relatively dense and highly absorbed regions (Lazzati et al. 2002). It is also possible that many dark bursts may be intrinsically weak sources, the faint tail of the GRBs luminosity distribution (De Pasquale et al. 2003), or sources with a very rapid decay (Groot et al. 1998) in the optical band.

The afterglow emission is seen to decay over time. In some bursts, a clear light curve steepening is observed after an interval of order days. The break is achromatic and typically attributed to the fact that the energy release is collimated in a jet. Other irregular temporal features are sometimes seen in bursts (see Zhang & Meszaros 2002, Zhang et al. 2005, Burrows 2005 and references therein): examples include a rebrightening in GRB 970508, wiggles in GRB 020104 and step-like features in GRB 030329. Also, “bump” features have been observed in several cases (e.g. GRB 970228, GRB 970508, GRB 980326, GRB 000203C) and various interpretations have been proposed, e.g., “refreshed shocks” (Panaitescu et al. 1998), supernova components (Bloom et al. 1999, Reichart 1999, Galama et al. 2000), dust echoes (Esin & Blandford 2002) or microlensing (Garnavich et al. 2000). On the other hand, signatures in the GRB lightcurve detected at earlier times may provide diagnostic information about the nature of the injection and eventually probe whether the energy is released impulsively during the event or more continuously during the immediate post-burst epoch (see e.g. Zhang & Meszaros 2002).

Until recently, most follow-up observations did not start until a few hours after the GRB, when the afterglow had already faded significantly. This situation has changed with the launch of the *Swift* mission, which provides both a rapid alert of GRB triggers to ground-based observers, and rapid X-ray and optical/UV follow-up observations of the burst afterglow. The *Swift* observatory (Gehrels et al. 2005) carries three science instruments: the Burst Alert Telescope (BAT; Barthelmy et al. 2005), which locates GRBs with 3' accuracy, the X-ray telescope (XRT, Burrows et al. 2005) and the Ultra-Violet Optical Telescope (UVOT, Roming et al. 2005a). When BAT detects a GRB trigger, *Swift* slews towards the source position within a few tens of seconds. Therefore, observations with the *Swift* instruments yield high quality data and cover the poorly investigated epoch occurring minutes after the burst. Interestingly, many GRBs localized and observed by *Swift* have shown no optical counterpart, even when optical observation started 100-200 s after the GRB onset. This provides evidence for a population of “intrinsically” dark GRBs (Roming et al. 2005b).

In this paper, we report the properties of the optically faint *Swift* GRB 050401, and discuss them in the light of the current models and scenarios of GRBs.

## 2 ANALYSIS OF THE $\gamma$ -RAY AND X-RAY DATA.

GRB 050401 triggered the BAT instrument at 14:20:15 UT on April 1, 2005 (Barbier et al. 2005, Angelini et al. 2005). The refined BAT position is RA=16<sup>h</sup>31<sup>m</sup>16<sup>s</sup>, Dec=2°11'35" with a position uncertainty of 3' (95% C.L., Sakamoto et al. 2005). The  $\gamma$ -ray band lightcurve started 9 s before the BAT trigger time and it shows 4 main peaks (see Figure 1). The peak count rate was 5000 counts/s (Barbier et al. 2005).

Analysis of the BAT data (15-350 keV energy band) yields a GRB duration  $t_{90} = 33$  s.

We use the mask-weighted technique to subtract the background in the BAT for spectral analysis, which is only effective up to 150 keV. *Swift* began to slew towards the source about 25 sec after the trigger, while the prompt emis-

sion was still active. We created separated BAT spectra and response matrices for the pre-slew and slew phases, and we fitted them jointly (see figure 2) with a simple powerlaw model. No significant improvement in  $\chi^2_\nu$  is found with a cutoff power-law model. Results are reported in the first entry of Table 1.<sup>1</sup>

The fluence detected by BAT in the 15 – 150 keV range is  $(8.6 \pm 0.3) \times 10^{-6}$  erg cm<sup>-2</sup>. Assuming a redshift of  $z = 2.9$  (see later) and a spherically symmetric emission, this corresponds to a  $\gamma$ -energy release of  $9.6 \times 10^{52}$  erg between 15 and 150 keV in the cosmological rest frame of the burst (derived by means of the ‘k-correction’ of Bloom et al. 2001). This result differs from that obtained by Chincarini et al. (2005), who reported an energy spectral index  $\beta = -0.13 \pm 0.05$  (using the 20-150 keV data) and a  $\gamma$ -energy release ( $\sim 2.8 \times 10^{53}$  erg) in the 15-350 keV band. However, we note that GRB 050401 prompt emission was also detected by Konus-Wind (Golenetskii et al. 2005). The Konus data (see below) suggest a steepening of the spectral index above  $E_0 \sim 150$  keV, which might explain the large difference between the two analyses.

As observed by the Konus-Wind instrument, GRB 050401 had a duration of  $\sim 36$  s and a fluence of  $(1.93 \pm 0.04) \times 10^{-5}$  erg cm<sup>-2</sup> in the 0.02-20 MeV band. Golenetskii et al. (2005) analyzed the spectrum gathered in the first 3 peaks (0-17 s after the trigger, first segment) and last peak (24.8-32 s after the trigger, second segment) separately (see again Table 1). We note that, if we adopt a cutoff powerlaw-model and fix the break energy  $E_0 = 150$  keV (as inferred from the Konus data), the spectral index obtained by *Swift*, which is averaged over the whole gamma-ray emission phase, is consistent with that obtained by Konus.

Observations were not possible with the *Swift* UVOT telescope because of the presence of a 4<sup>th</sup> magnitude star in the field of view, while XRT started observations about 130 s after the trigger. An unknown bright X-ray source was detected at R.A. = 16<sup>h</sup> 31<sup>m</sup> 29<sup>s</sup>, Dec = 02° 11' 14", within 42 arcseconds of the initial BAT position (Angelini et al. 2005); the coordinates were later confirmed by ground processing. This source subsequently faded, indicating that it was the X-ray counterpart of GRB 050401.

The first data were taken with the XRT (Hill et al. 2005) in its Imaging Mode (IM), then followed by a segment of data in the PhotoDiode mode (PD). After that, because of the bright star near the edge of the XRT field of view, the detector continuously switched between Windowed Timing (WT) and Photon Counting (PC) mode. The initial PC mode data were piled-up and we did not include them in the analysis. In the first day of observation, *Swift* observed the X-ray afterglow until 5.6 hours after the trigger. More follow-up observations were performed 4.43-6.38 and 6.48-12.33 days after the trigger. The total exposure time is about 48 ks, divided into 21 ks in WT mode and 27 ks of PC mode (including piled-up data).

Analysis of XRT data was performed using the XRT pipeline software. The accumulated DN in the IM data were converted to a count-rate following the method of Hill et al.

<sup>1</sup> Throughout this paper, we report errors at  $1\sigma$ , unless otherwise indicated

2005. The PD mode data points have been obtained by subtracting the contribution of the corner calibration sources. As for the WT mode data, the extraction regions for the source and for the background consist of boxes of 60x40 pixels. The source and background extraction regions for the PC data are circles of 20 pixel and 60 pixel radius, respectively. We considered the 0-2 grade events for the WT mode and 0-12 for the PC mode, which cover events up to 4 pixels in size. For the spectral analysis, we generated the physical ancillary response matrices with the task *xrtmkarf*, while the response matrices (RMs) were retrieved from the latest *Swift* calibration database, CALDB 20050601 (<http://heasarc.gsfc.nasa.gov/docs/heasarc/caldb/swift/>). At the time of writing, these RMs are considered as the most reliable, basing on comparison with spectra of calibration sources. We only considered data taken with CCD detector temperature  $T < -48$  C.

We restricted both the spectral and temporal analysis to counts within the 0.4-10 keV band since, at the time of writing, a good calibration of both WT and PC data is available in this band. Data were rebinned in energy by requiring a minimum of 15 counts per bin.

The X-ray lightcurve is shown in Figure 3. The presence of a break is clearly evident: if we try to fit the whole lightcurve with a single powerlaw, we get an unsatisfactory result ( $\chi^2_\nu = 904/114$ ), while the use of a broken powerlaw model ( $At^{\alpha_1}$  for  $t \leq t_b$ ;  $At_b^{\alpha_1 - \alpha_2} t^{\alpha_2}$  for  $t \geq t_b$ ) gives a statistically significant improvement ( $\chi^2_\nu = 129/112$ ). In this case, the best fit parameters are: decay indices  $\alpha_1 = -0.63 \pm 0.02$  and  $\alpha_2 = -1.46 \pm 0.07$  (before and after the break, respectively) and break time  $t_b = 4900 \pm 490$  s<sup>2</sup>. The break time is consistent with that reported by Chincarini et al. (2005), who report  $\sim 1300$  s corrected for cosmological time dilation, i.e. their break time has been divided by  $(1+z)$ . We also tried to fit the lightcurve with a smoothly joined broken power law model (Beurmann et al. 1999), to determine the "sharpness" of the X-ray lightcurve break. However, we found that data do not allow us to discriminate between a smooth and a sharp transition.

A fit of the WT spectral data taken before the lightcurve break time with an absorbed power-law model reveals a considerable amount of absorption,  $N_H^{tot} = (1.5 \pm 0.1) \times 10^{21}$  cm<sup>-2</sup>, clearly in excess of the Galactic value reported by Dickey & Lockman (1990),  $N_H^{Gal} = 4.85 \times 10^{20}$  cm<sup>-2</sup>, and the value inferred from the Galactic extinction map of Schlegel et al. (1998),  $N_H^{Gal} = 3.6 \times 10^{20}$  cm<sup>-2</sup> (in this case the extinction,  $A_V = 0.2$  has been converted to  $N_H^{Gal}$  using results by Predehl and Schmitt 1995).

In order to better estimate the column density corresponding to the circumburst medium only, we repeated the fit by accounting separately for the Galactic and extragalactic absorption columns, the latter rescaled at  $z = 2.9$ . We fixed the Galactic absorption to the Dickey & Lockman (1990) value. This gives an extragalactic column density of  $N_H \equiv N_H^{tot} - N_H^{Gal} \approx (1.7 \pm 0.2) \times 10^{22}$  cm<sup>-2</sup> (see Table 1; spectrum and best fit model are shown in Figure 4). To assess the robustness of this detection, we then repeated the fit without adding the extragalactic component, obtaining

a  $\chi^2_\nu = 405/262$ . This means that accounting for the extra absorption  $N_H$  produces a statistically significant improvement. The F-test has also been widely used to test the significance of a spectral component, although, when applied to parameters such as  $N_H$  (which is bounded to be  $> 0$ ) this may be inappropriate in a strict sense (see Protassov et al. 2002). For completeness, we report that we checked the F-test statistic, obtaining a value of 117 with a probability that the improvement is due to chance of  $\sim 10^{-22}$ .

We find no evidence for spectral evolution: parameters consistent with those given above are obtained when fitting the spectra taken before and after the 4900 s break. An analysis of the PC spectrum with the same spectral model also does not show any significant difference in the spectral parameters (see Table 1). When compared to the X-ray afterglows detected by other observatories, like *BeppoSAX*, *Chandra* and *XMM-Newton*, the afterglow of GRB 050401 appears to be a moderately bright source: the 1.6-10 keV X-ray flux normalized at 11 hours after the burst is  $(2.3 \pm 0.2) \times 10^{-12}$  erg cm<sup>-2</sup>s<sup>-1</sup> (see Berger et al. 2003, Roming et al. 2005b, De Pasquale et al. 2005).

### 3 FOLLOW-UP OBSERVATIONS IN DIFFERENT ENERGY BANDS

Although the *Swift* UVOT could not observe at the GRB position, a series of ground-based optical follow up observations was performed, triggered by the prompt *Swift* localization.

The afterglow was first identified by Rykoff et al. (2005), who detected it in images taken shortly after the GRB. Later, following the distribution of the BAT trigger, the BAT error circle was imaged with the 40-inch telescope at Siding Spring Observatory. These observations consisted of two unfiltered 120 s exposures, followed by 41 *R*-band 240 s exposures. Data showed a faint fading source, at coordinates RA=16:31:28.81, Dec=+02:11:14.2 (J2000), i.e. within the XRT error circle. This object was not present on the Digitised Sky Survey plates (McNaught et al. 2005).

The rapid distribution of the afterglow position, along with a finding chart, enabled other follow-up observations including some spectroscopic ones. Fynbo et al. (2005) reported the detection of a system of absorption lines in the optical spectrum detected with FORS2 at the Very Large Telescope, indicating a redshift of  $z = 2.9$ . Other observations followed, up to  $\sim 0.5$  days after the GRB onset. The full list is summarized in Table 2 and the optical light curve is shown in Figure 3. We found that the optical decay law is not consistent with a single powerlaw ( $\chi^2 = 24.8$  for 13 d.o.f.). We caution that the optical light curve has been obtained by observations performed by different facilities, which used diverse calibrations. In particular, the photometry of all exposures taken with the Siding Spring Observatory is relative to the first *R*-band image, which was then calibrated to match the USNO-A2.0 catalogue red magnitude. Because of this, although the relative magnitudes are accurate, the overall normalization can only be considered to be accurate at the  $\sim 0.5$  mag level. ARIES measurements also refer to USNO-A2.0 stars, while the Maidanak estimate is based on stars of the similar USNO-B2.0 catalogue, and D'Avanzo et al. 2005, and Greco et al. 2005 data used the Landolt catalogue. Therefore some systematic bias may well

<sup>2</sup> We note that at the time of the slope change *Swift* was not observing the GRB.

be present. However, taken at face value the combined data suggest a non-monotonic decaying behaviour. We note that the decay slope in the first 10000 s (first part of the Siding Spring data), is  $\alpha_0 = -0.68 \pm 0.06$ , consistent with the first X-ray decay. The Siding Spring data are not consistent with being constant. A powerlaw fit to these data in isolation gives  $\alpha = 0.56 \pm 0.2$ . The case  $\alpha = 0$  can be rejected at the  $2.5\sigma$  confidence level.

## 4 DISCUSSION.

### 4.1 The break in the X-ray light curve.

As we have seen, the X-ray light curve of GRB 050401 registered with XRT shows an initial decay slope of  $\alpha_1 = -0.63 \pm 0.02$ , which steepens at  $\sim 4900$  s. After this time, the source fades with a slope of  $-1.46 \pm 0.07$ .

In principle, there are several physical mechanisms that can dictate the physical behavior of the afterglow during its initial decline and can produce a break at these early times. For instance, as described by Sari et al. (1999) and Rhoads et al. (1999), a break in the light curve is expected if the fireball outflow is not spherically symmetric but collimated within a jet. Such an effect has been invoked to explain breaks in Gamma-Ray Burst afterglow light curves in several cases (see, for example, Sari et al. 1999, Panaitescu & Kumar 2002, Frail et al. 2003). However, we suggest that this explanation is not applicable to the case at hand, for at least two reasons. First, according to the fireball model of GRB afterglows, the observed temporal decay index and spectral slope should be linked through the so-called closure relation (see e.g. Price et al. 2002). This relation depends on the kind of expansion (spherical or jet), on the density profile of the medium (uniform or wind) and on the cooling state of the electrons responsible for the synchrotron emission. In particular, for jet-like emission it should be  $\alpha = 2\beta - 1$  or  $\alpha = 2\beta$  depending on whether the cooling frequency  $\nu_c$  is above or below the X-ray frequency  $\nu_X$  (see Sari et al. 1999). In the case at hand, we find  $\beta = -0.9 \pm 0.03$  (the spectral index is not supposed to change after the beginning of the jet expansion phase) and  $\alpha = -1.42 \pm 0.07$  (decay index after the break), so none of the above closure relations is satisfied. Second, if interpreted within the jet break scenario the observed parameters are not compatible with the relation between the peak energy and the (collimation corrected)  $\gamma$ -ray energy release proposed by Ghirlanda et al. (2004). In fact, by using  $E_{\gamma,iso} = 3.5 \times 10^{53}$  erg (as inferred from Konus data) and  $t_b = 4900$  s we obtain a jet opening angle  $\theta \simeq 1^\circ$  (see expression 1 in Ghirlanda et al. 2004). In turn, this corresponds to a collimation corrected energy  $E_\gamma = 4.8 \times 10^{49}$  erg and to a peak energy in the cosmological rest frame of  $E_{peak} = 56$  keV, in clear disagreement with the value inferred by Konus data ( $\sim 500$  keV).

Another potential reason for a break in the light curve is that the energy release is spherically symmetric, but the X-ray observation occurs while  $\nu_c$  passes through the X-ray band, causing the light curve to steepen by 0.25 (see Sari et al. 1999). However, in this case we should also observe a steepening of 0.5 in the spectral slope while there is no evidence for that across the break of GRB 050401. Moreover, a change of 0.25 is not sufficient to account for the steepening in the light curve.

On the other hand, we find that both the initial shallow decay and the break can be explained by a model in which the central engine continues to inject radiative energy into the fireball for several thousands of seconds. This scenario has been investigated by Zhang & Meszaros (2001) and Zhang & Meszaros (2002). By assuming a source luminosity law of the kind  $L \propto t^q$ , where  $t$  is the intrinsic time of the central engine (or the observer's time after the cosmological time dilation correction), these authors found that continuous injection of energy influences the fireball and the observed light curves as long as  $q > -1$ . In this case, the spectral and decay slopes are linked through the relation:

$$\alpha = (1 - q/2)\beta + q + 1, \quad (1)$$

which holds if the observed X-ray frequency is between the synchrotron peak frequency and the cooling frequency (see later). By using the observed values of  $\alpha$  and  $\beta$ , we obtain  $q \sim -0.5$  and  $q \sim -1$  before and after the break time, respectively. The latter is consistent with no injection (since  $q < -1$  does not influence the fireball dynamics), while before the time break the central engine injects energy with a luminosity law  $L \propto t^{-0.5}$ . The change in the decay slope occurs at the point when the central engine ceases to inject significant amounts of energy. We note that the decay slope of the optical and the X-ray flux before the breaks are consistent within the errors. This is in agreement with the continuous injection model, as long as the optical and the X-ray band belong to the same spectral segment.

There is variant to this scenario, which is observationally undistinguishable, i.e. a model in which the central engine activity is as brief as the prompt emission itself but, at the end of the prompt phase, the ejecta are released with different velocities (Lorentz factors, see Panaitescu et al. 2005). The fastest shells initiate the forward shock, decelerate, and are successively caught by the slowest shells. The consequent addition of energy in the blast-wave mitigates the deceleration and the afterglow decay rate. Assuming that the mass  $M$  of the ejecta follows the law

$$M(>\gamma) \propto \gamma^s, \quad (2)$$

where  $\gamma$  is the Lorentz factor, one can find an effective  $s$  value that mimics the effect of non vanishing  $q$  index in the luminosity law. By following Zhang et al. (2005), this is:

$$s = -(10 + 7q)/(2 - q), \quad (3)$$

therefore, the value  $q = -0.5$  inferred above is equivalent to an  $s$ -index of  $s = -2.6$ . This explanation has been proposed, for example, to explain the initial mild decline of the optical light curve of GRB 010222, which shows a decay slope of  $\alpha_O = -0.7$  (Stanek et al. 2001, Bjornsson et al. 2002) for  $\sim 10$  hours after the trigger, followed by a break and a steeper decay. Bjornsson et al. (2004) also proposed that injection of energy by slow shells could explain the wiggles in the light curve of GRB 021004.

In the case of GRB 050401, it is noteworthy that a possible optical rebrightening seems to take place shortly after the change of the slope of the X-ray. In the framework of the continuous energy injection model, this could be explained by the onset of a "reverse shock". The basic idea is that, after the end of the injection phase, a reverse shock wave crosses the whole ejecta, heating them and causing a peak in the emission. After that, the shocked ejecta start to cool

adiabatically once again. However, in order to assess this issue a more detailed model investigation is required, which is beyond the scope of this work.

As previously discussed, the analysis of the X-ray data taken after the break is consistent with a scenario in which a "standard" fireball expands in a constant density medium, provided that the observed X-ray band lies between the synchrotron peak frequency and the cooling frequency. Following Sari et al. (1999), the closure relation should in this case read  $\alpha = (3/2)\beta$ , which is satisfied within  $1\sigma$ . One possible complication is that, if the fireball expands in a medium with constant density, the cooling frequency is expected to decrease with time according to  $\nu_C \propto t^{-1/2}$ . Accordingly, in most X-ray afterglows, the cooling frequency is already between the peak frequency and the X-ray observing frequency less than 1-2 days after the GRB onset. In contrast, our data seems to suggest that in the case of GRB 050401 the cooling frequency remains above the X-ray frequency for about  $10^6$  s. While this may be explained in terms of relatively low values of magnetic field energy ( $\epsilon_B$ ) and density (see Sari et al. 1999), we also note that a transit of the cooling frequency through the X-ray band after 20,000 s cannot be completely excluded by our data: the change in the decay slope and in the spectral slope would be 0.25 and 0.5 respectively, and hence difficult to detect due to very low statistics in the late time XRT detections of the afterglow.

## 4.2 The optical and X-ray properties of GRB 050401.

The GRB 050401 afterglow is quite bright in the X-ray band, but weak in the optical, with an optical to X-ray flux ratio similar to those of 'dark bursts'.

In order to compare its properties with those typically observed in other GRBs, we show in figure 5 the relation between the optical and X-ray fluxes for a series of GRB afterglows detected by *BeppoSAX*. As pointed out by several authors (e.g. De Pasquale et al. 2003, Roming et al. 2005b), the GRBs with optical counterparts exhibit a correlation between the fluxes in these two spectral bands. Several GRBs without optical counterparts also show an X-ray emission consistent with that expected by assuming the validity of the same correlation, indicating that they may well be simply the faint tail of the same population. However, there is evidence for a sample of dark GRBs which have "normal" X-ray fluxes but with tight upper limits in the optical. Jakobsson et al. (2004) reached similar conclusions by comparing the spectral index between the optical and the X-ray band,  $\beta_{OX}$ , with the expectations of the fireball model, which requires  $\beta_{OX} \leq -0.5$ . They found that at least 10 % of the events in their sample had  $\beta_{OX} > -0.5$ , and called them the *truly* dark GRBs. To explain the optical faintness of these bursts, two main scenarios have been proposed. The first idea is that they occur at very high redshift, possibly following the death of Population II and III stars (Bromm & Loeb 2002), in which case the optical flux is washed out by the intervening Ly- $\alpha$  forest. The second idea is that dark GRBs have lines of sight passing through large and giant molecular clouds (hereafter GMCs). GMCs are rich in dust, which extinguishes optical and UV light very efficiently.

GRB 050401 appears to be an 'intermediate' case. An optical afterglow is detected, but is very faint relative to its

X-ray flux compared to other GRBs with optical counterparts. Its optical to X-ray spectral index is  $\beta_{OX} = -0.33$ , which makes this source a dark burst according to Jakobsson et al. (2004) classification. Given the detection of an optical counterpart with a likely redshift of  $z = 2.9$ , we can exclude the hypothesis of a very high redshift. On the contrary, the X-ray spectrum indicates a high absorption, typical of GMCs (Reichart & Price 2002, Galama & Wijers 2001).

Therefore, a natural question is: can the hypothesis of extinction in this medium explain the weakness of the optical emission detected? The light detected at Earth in the R band (centered at 700 nm) was emitted at a wavelength of 180 nm in the GRB cosmological restframe at a redshift of  $z = 2.9$ . The simplest working hypothesis is to assume that the same medium is responsible for both the X-ray and optical extinction. In this case, the hydrogen column density measured from the X-ray spectrum ( $N_H = 1.7 \times 10^{22} \text{ cm}^{-2}$ ) would correspond to an absorption in the V band of  $A_V = 10$  magnitudes (Zombeck 1990). Assuming a Galactic extinction curve of  $A_\lambda/A_V \propto \lambda^{-1}$ , this results in a predicted extinction of  $A_\lambda \sim 30$  magnitude for  $\lambda = 180$  nm. This value is unreasonably high and would imply that the optical afterglow was unrealistically bright. Thus we can exclude this simple explanation.

Instead, comparing with the optical-to-X-ray flux ratio typical of other 'non-dark' GRBs (De Pasquale et al. 2003, Jakobsson et al. 2004, Roming et al. 2005b) we could expect a plausible extinction of about 3 magnitudes, which is clearly not in agreement with the measured X-ray absorption when we adopt the Galactic extinction curve. We note that a discrepancy like this has been noted in several other cases (for a summary, see Stratta et al. 2004), but for GRB 050401 we have the advantage of a fairly constrained value of the absorption parameter.

In order to reconcile the value of absorption with the likely extinction, a few hypothesis have been proposed. The first scenario involves the presence of a gas-to-dust ratio much lower than the Galactic one and/or a dust grain size distribution skewed toward large grains (Stratta et al. 2004). This first case is, for instance, typical of dwarf galaxies like the Small Magellanic Cloud (SMC). In fact, for the SMC interstellar medium (ISM) a dust content  $\sim 1/10$  of the Galactic one has been inferred (Pei et al. 1992). Thus, we would have  $\sim 3$  magnitudes of extinction based on the measured value of the X-ray absorption. This value is close to that required. We note, however, that the best-fit  $N_H$  value has been obtained by assuming Galactic metal abundances, while the metallicity of SMC is  $1/8$  of the Milky Way (Pei et al. 1992). If this low metallicity were adopted, we would need to adjust the value of  $N_H$  upwards by a factor of  $\sim 7$ , given that the majority of the absorption in the X-ray band is produced by heavy elements, so this is not a solution.

Another scenario that could result in a low  $A_V/N_H$  is that there is a change in both the gas-to-dust ratio and the distribution of grain size, with the latter enriched in large grains by the effects of the high-energy radiation of the GRBs. Dust grains can be heated and evaporated by the intense X-ray and UV radiation fields up to  $\sim 20$  parsecs from the GRB (Waxman & Draine

2000, Draine & Hao 2002, Fruchter et al. 2001). Perna et al. (2003) and Perna & Lazzati (2002) show that the consequence of exposing dust to intense radiation fields can be a grain size distribution flatter than the original one. The main reason is that dust destruction is more efficient on small grains. Perna et al. (2003) computed the extinction curve that is obtained if standard Galactic dust is exposed to a GRB and found that the extinction curve can be very flat, at least for bursts lasting more than a few tens of seconds.

Finally, a distribution of grain size skewed toward large grains can also be produced by an efficient mechanism of coagulation of smaller grains in a dense environment (Kim & Martin 1996, Maiolino et al. 2001), in which case the dust-to-gas ratio is unaffected. Both of the above explanations could lessen the discrepancy between the low UV extinction and the high X-ray absorption detected.

## 5 CONCLUSIONS.

We have presented *Swift* observation of the Gamma-Ray Burst 050401 and we have discussed the properties of the prompt emission, and, in more detail, the X-ray afterglow. The light curve of this burst shows a break 4900 s after the trigger, changing from a decay index of  $\alpha_1 = -0.63$  to  $\alpha_2 = -1.46$ , while the spectral energy index does not change. To explain this behavior, we have proposed that the 'central engine' has been active until the time of the break, with luminosity described by the law  $L \propto t^{-0.5}$ . Another possibility is that the central engine activity turned off as the prompt emission ended, but the shells had a broad distribution of Lorentz factors. In this case, the slowing front of the GRB blastwave is continually re-energized by the arrival of progressively slower shells and the flux decay is therefore mitigated. We find that the decay slope observed before the break may be reproduced if the shells were emitted with a powerlaw distribution of Lorentz factor,  $M \propto \gamma^{-2.6}$ . The peculiar behaviour of the optical light curve can be in agreement with the two scenarios proposed.

After the break time, the profiles of the X-ray light curve and spectrum are consistent with those expected when a fireball expands in a circumburst medium with constant density, and the observed X-ray band lies between the synchrotron peak frequency and the cooling frequency.

Even though the X-ray flux of the GRB 050401 afterglow is high, the optical counterpart is faint. This leads to a low optical to X-ray flux ratio similar to that of dark GRBs which are likely to be obscured by some mechanism. The spectral analysis shows clear evidence of absorption, namely  $N_H = (1.7 \pm 0.2) \times 10^{22} \text{ cm}^{-2}$ , at the redshift  $z = 2.9$  of the GRB. This value is typical of giant molecular clouds where star forming regions are located. The detection of a dense circumburst medium could lead us to the conclusion that this "obscuration mechanism" is, at least in this case, extinction.

However, the amount of extinction extrapolated by assuming the Galactic extinction law is far too high to be physically acceptable. This may be evidence that the circumburst medium is characterized by a dust grain size distribution different from the Galactic one, and skewed towards large grains. This could be due either to coagulation of smaller

grains or to small dust grain destruction due to high energy photons produced by the GRB. In the latter case the dust-to-gas ratio would also be different from the Galactic one.

Acknowledgements: We are grateful to an anonymous referee for his/her suggestions that led to a substantial improvement of the draft. APB, KPA acknowledge support for this work at Leicester by PPARC. SZ also thanks PPARC for support through an Advanced Fellowships.

## REFERENCES

- Angelini L. et al., 2005, GCN 3161
- Barbier et al., 2005, GCN 3162
- Barthelmy S.D. et al., 2005, Sp. Science Rev, in press
- Beuermann K. et al. 1999, A&A, 352, L26
- Berger E. et al., 2003, ApJ, 590, 379.
- Berger E. et al., 2005, ApJsubmitted, (astro-ph/0505107)
- Bjornsson G., Hjorth J., Pedersen K. et al., 2002, ApJ, 579L, 62.
- Bjornsson G., Gudmundsson E.H. & Johannesson G., 2004, ApJL, 615, 77.
- Bloom J.S. et al., 1999, Nature, 401, 453
- Bloom J.S, Frail D.A., Kulkarni S.R. et al., 2001, ApJ, 508, L21
- Bromm V. & Loeb A., 2002, ApJ, 575, 111
- Burrows D. et al., 2005, Space Science Review, in press
- Chincarini et al. 2005, submitted to ApJ, astro-ph/0506453
- D'Avanzo P. et al., GCN 3171
- De Pasquale M., Piro L., Perna R. et al. 2003, ApJ, 592, 1018
- Dickey J.M. & Lockman F.J., 1990, ARAA, 28, 215
- Draine B.T. & Hao L., 2002, ApJ, 569, 780
- Esin, A.A. & Blandford, R., 2000, ApJL, 534, L51
- Frail D. 2003, IAU Colloquium 192, Supernovae: 10 Years of 1993J Valencia, astro-ph/0309557
- Frontera F. et al., 2000, ApJ, 127 59
- Fruchter A.S. et al., 2001, ApJ, 563 597
- Fynbo J. et al., 2005, GCN 3176
- Fruchter A.S., 1999, ApJ, 512L 1
- Galama, T.J., et al., 2000, ApJ, 536, 185
- Galama, T.J. & Wijers, R.A.M.J. 2001, ApJL, 549, L209
- Garnavich, P., Loeb, A. & Stanek, K., 2000, ApJL, 544, 11
- Gehrels N. et al., 2005, ApJ, 621, 558
- Ghirlanda G., Ghisellini G. & Lazzati D., 2004, 616, 331.
- Golenetskii S. et al., 2005, GCN 3179
- Greco G. et al., 2005, GCN 3319
- Groot P.J, Galama T.J., Vreeswijk P.M. et al. 1998, ApJ, 502L 123
- Hill J.E. et al., 2005, in preparation
- Jakobsson P. et al., 2004, ApJL, 617, L21
- Kim S.H. & Martin P.G., 1996, ApJ, 462, 296
- Lamb, D.Q. et al., 2005, New Astronomy Reviews, 48, 423
- Lazzati D. et al. 2002, MNRAS
- Maiolino R. et al., 2001, A&A, 365, 37
- Misra K. et al. 2005, GCN 3175
- McNaught R. et al., 2005, GCN 3163
- Panaitescu A., Mészáros, P. & Rees, M.J., 1998, ApJ, 503, 314
- Panaitescu A. & Kumar P., 2002, ApJ, 779, 789

- Panaitescu A. et al., 2005, MNRAS submitted, astro-ph/0508340
- Pei Y.C. et al., 1992, ApJ, 395, 130
- Perna R. & Lazzati D., 2002, ApJ, 580, 261
- Perna R. et al., 2003, ApJ, 585, 775
- Predehl P. & Schmitt J.H.M.M., 1995, A&A, 293, 889
- Price P. et al., 2002, ApJL, 572, L51
- Price P. et al., 2005, GCN 3164
- Protassov R., van Dyk D.A., Connors A. et al. 2002, ApJ, 571, 545
- Reichart E., 1999, ApJL, 521, L111
- Reichart E. & Price P., 2002, ApJ, 565, 174
- Rhoads J. et al., 1999, ApJ, 525, 737
- Roming P. et al., 2005a, Space Science Review, in press
- Roming P. et al., 2005b, to be submitted to Science, astro-ph/0509273
- Rykoff E. S. et al., 2005, accepted by ApJL, astro-ph/0508495
- Sari R. et al., 1999, ApJL, 519, 17
- Sakamoto T., 2005, private communication.
- Schlegel D.J., Finkbeiner D.P & Davis M, 1998, ApJ, 500, 525S
- Soderberg A.M. et al., 2005, GCN 3187
- Stratta G. et al., 2004, ApJ, 608, 846
- Stanek K., Garnavich P.M, Saurabh J., et al., 2001, ApJ, 563, 592.
- Waxman E. & Draine B.T., 2000, ApJ, 537, 796
- Zahharov. et al., 2005, GCN 3174
- Zhang B., Fan Y.Z., Dyks J. et al., 2005, submitted to ApJ, astro-ph/0508321
- Zhang B. & Meszaros P., 2001, ApJ, 552L, 35
- Zhang B. & Meszaros P., 2002, ApJ, 566, 712
- Zombeck M., 1990, Handbook of Astrophysics, Ed. Cambridge University Press

Instrument	Section	$\beta$	$\beta_1$	$E_0$	$N_H$ ( $10^{22}$ )	$\chi^2_\nu$
Swift:	BAT Prompt Emission	$-0.53 \pm 0.07$				136/115
	WT pre-break	$-0.9 \pm 0.03$			$1.7 \pm 0.2$	280/261
	WT post-break	$-0.9 \pm 0.13$			1.7	16.3/21
	PC	$-0.75 \pm 0.15$			1.7	21.8/18
<hr/>						
Konus-Wind:	first segment	$-0.15 \pm 0.16$	$-1.65 \pm 0.31$	$156 \pm 45$		
	second segment	$+0.17 \pm 0.21$	$-1.37 \pm 0.14$	$119 \pm 26$		

**Table 1.** Values of the parameters for the spectral fit of GRB 050401. Swift data have been fitted with a simple power-law model (energy index  $\beta$ ) and divided into four sections: prompt emission, WT data before the break in the light curve, WT data after the break, PC data. For the latest two sections,  $N_H$  has been kept fixed to the value obtained from the WT pre-break data. Errors are at 68% confidence level. For comparison, we also reported the results of the fitting of Konus-Wind prompt emission data performed by Golenetskii et al. (2005). A Band model has been adopted by these authors, so in this case  $\beta$ ,  $\beta_1$  are the low and high energy indices and  $E_0$  is the break energy.

Time after GRB (days)	R magnitude	Reference
0.040	$21.05 \pm 0.3$	Siding Spring Observatory
0.043	$21.25 \pm 0.3$	"
0.051	$20.85 \pm 0.2$	"
0.055	$21.35 \pm 0.3$	"
0.063	$21.85 \pm 0.4$	"
0.071	$21.55 \pm 0.3$	"
0.086	$21.55 \pm 0.2$	"
0.102	$21.85 \pm 0.3$	"
0.126	$21.85 \pm 0.3$	"
0.149	$21.85 \pm 0.4$	"
0.173	$22.05 \pm 0.3$	"
0.24	$21.27 \pm 0.2$	Misra et al. 2005 (GCN 3175)
0.39	$21.97 \pm 0.2$	Kahharov et al. 2005 (GCN 3174)
0.46	$22.47 \pm 0.4$	Greco et al. 2005 (GCN 3319)
0.47	$22.95 \pm 0.1$	D'Avanzo et al. 2005 (GCN 3171)

**Table 2.** Log of GRB 050401 Optical observations. Values quoted in this table have been corrected for Galactic extinction. As explained in the text, the zero-points for these observation might be uncertain for  $\sim 0.5$  magnitude due to USNO-A2.0 calibration.



Maskweighted 1 s Lightcurve

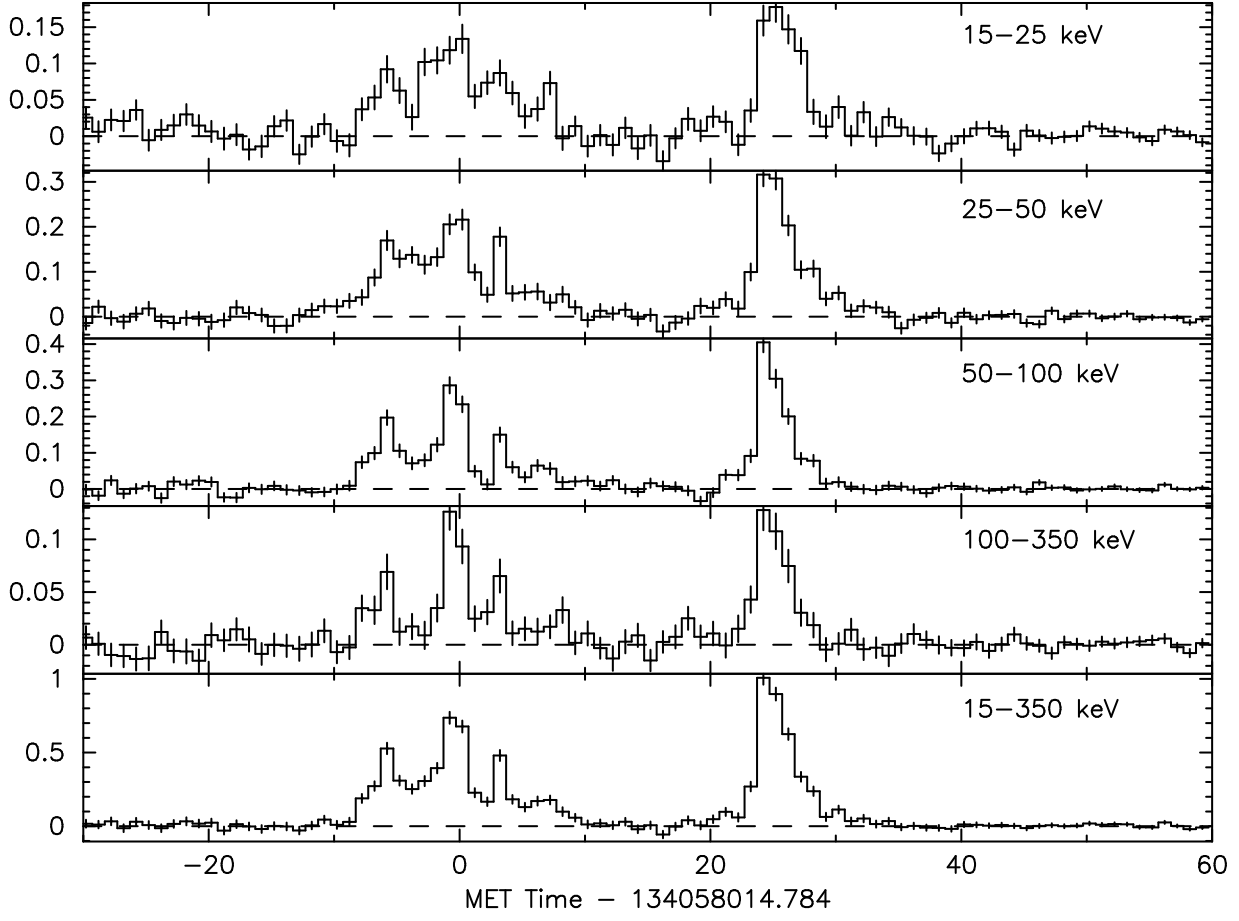


**Figure 1.** GRB 050401 light curve in Gamma-Rays. On the Y-axis we show the background subtracted count/s per fully illuminated detector for an equivalent on-axis source.

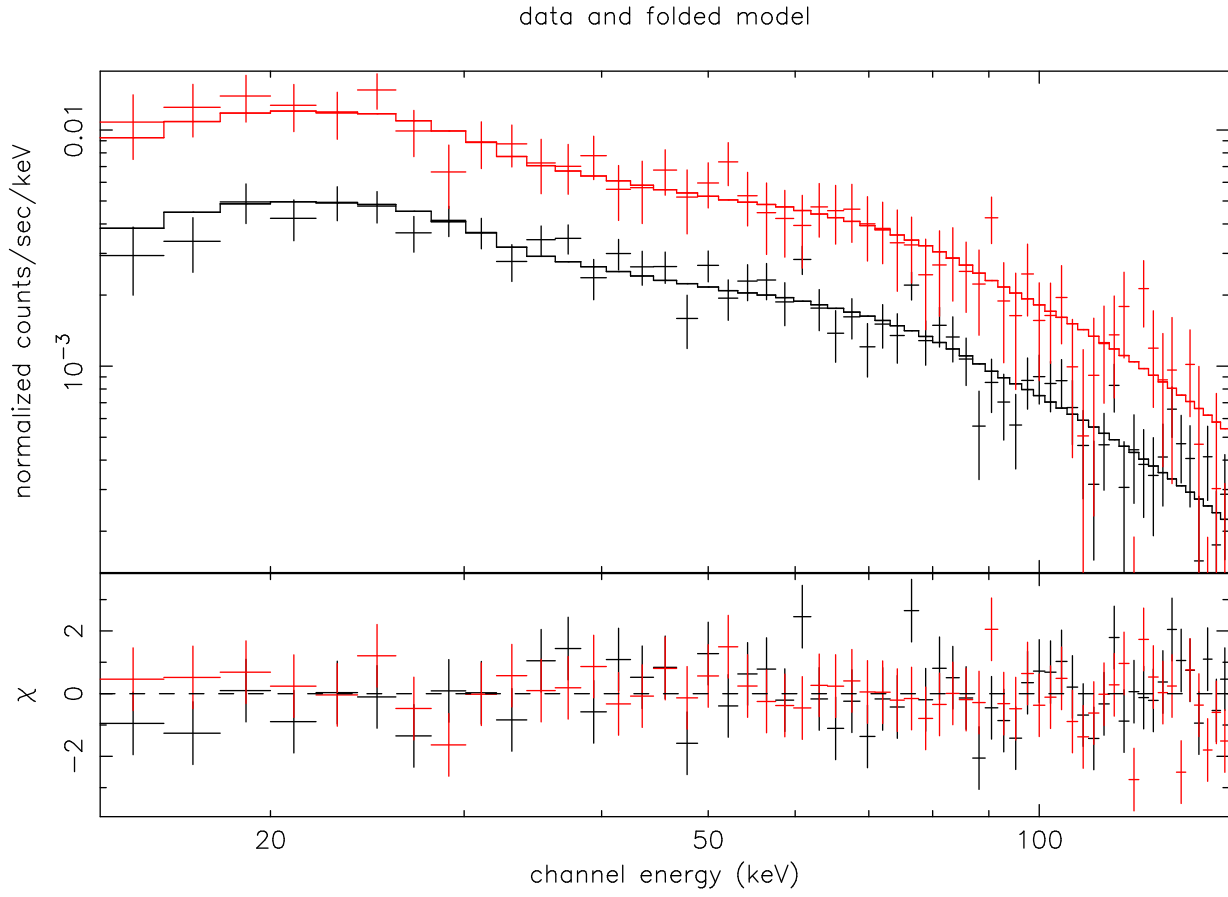


**Figure 2.** GRB 050401  $\gamma$ -ray spectrum detected by BAT before (red colour) and during the slew (black). Both spectra are consistent with the same fitting power law model, plotted as a solid line (see first entry in Table 1).

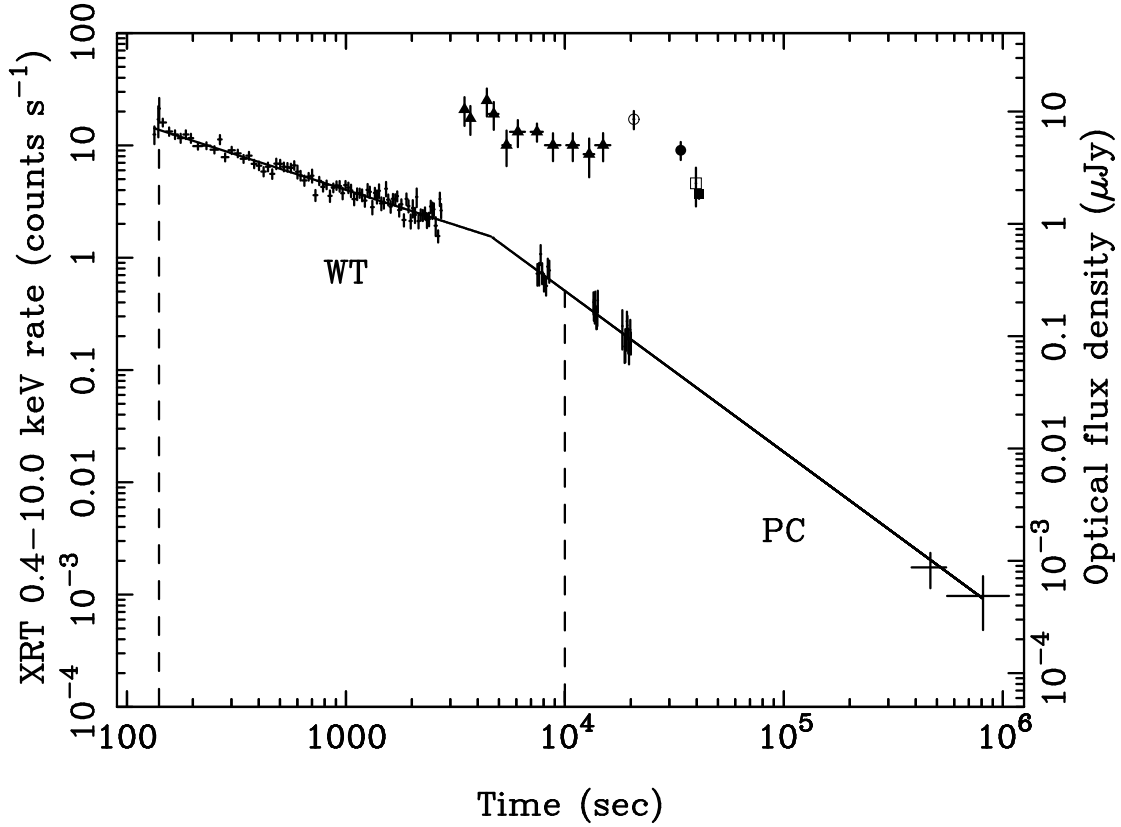


**Figure 3.** GRB 050401 afterglow light curves. The crosses represent the X-ray light curve registered with XRT (0.4-10 keV band). The first point is taken in Image mode, followed by 2 Photodiode points. After that, data have been taken in Windowed Timing (WT) mode from 0.14 up to 9 ks after the trigger (section between the two vertical dashed lines), and in Photon Counting (PC) mode from 13.6 up to 1050 ks after the trigger. The optical afterglow light curve is plotted in the upper part of the figure. Triangles: Siding Spring data. Circle: ARIES (Misra et al. 2005) data. Filled circle: MAO (Kahharov et al. 2005). Square: Bologna (Greco et al. 2005) data. Filled square: TNG (D’Avanzo et al. 2005) data.

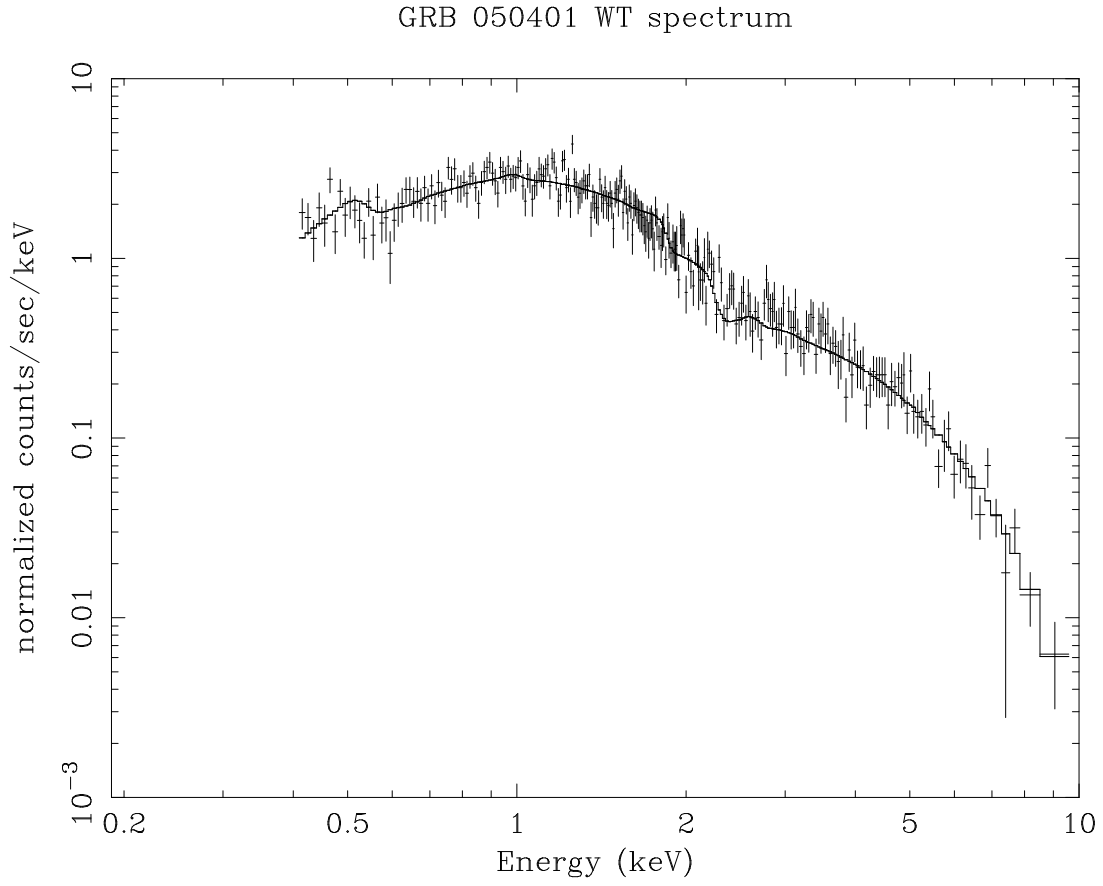


**Figure 4.** GRB 050401 X-ray spectrum registered with XRT in WT mode before the break. The solid line is the best fitting absorbed power-law model (see text and Table 1 for details).

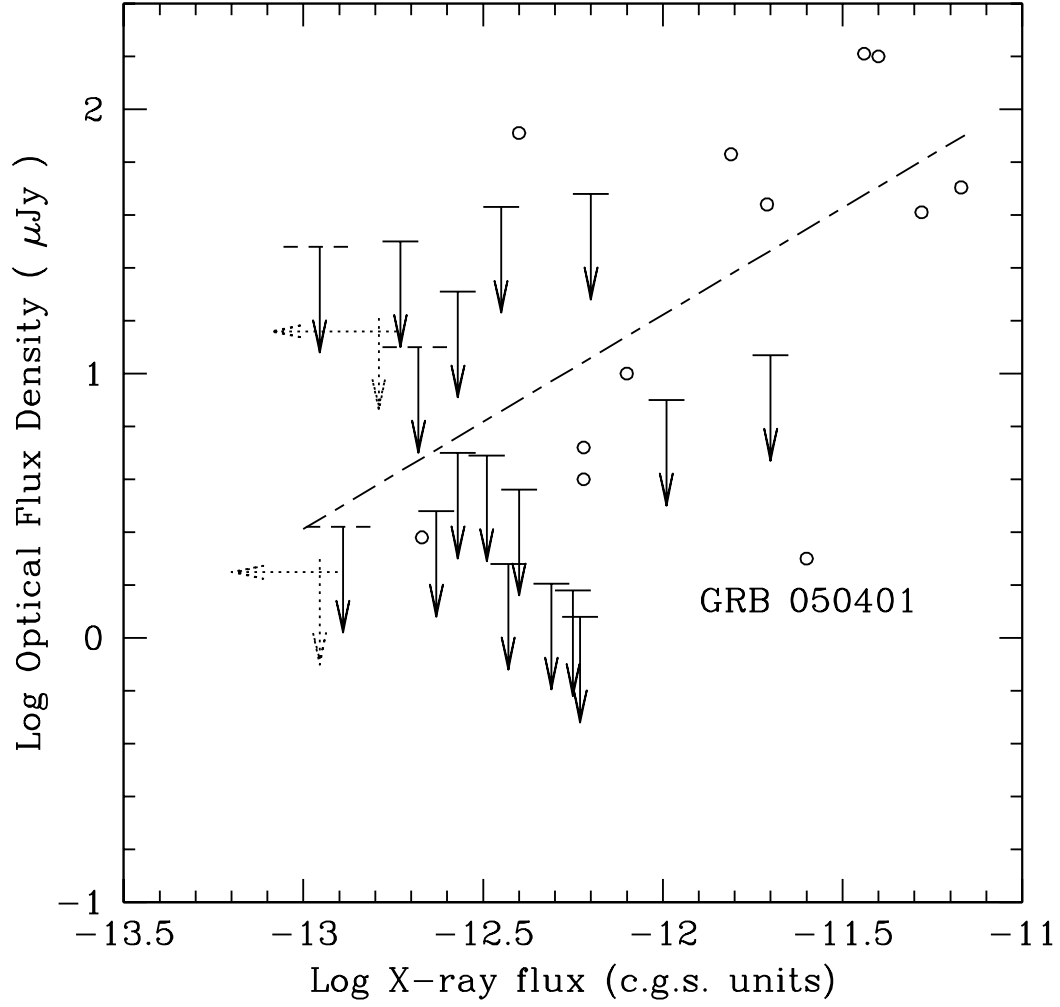


**Figure 5.** Optical vs. X-ray flux of GRB 050401 afterglow compared to *BeppoSAX* GRBs. Open Circles: GRBs with optical counterpart. Solid arrows: GRBs without optical counterpart. Dashed arrows: doubtful afterglows. Dotted arrows: upper limits. Short-long dashed line: best fit of optical vs. X-ray flux (adapted from De Pasquale et al. 2003).